

Serial Sectioning Methods for Generating 3D Characterization Data of Grain- and Precipitate-Scale Microstructures

Michael D. Uchic

Abstract This chapter provides an overview of the current state-of-the-art for experimental collection of microstructural data of grain assemblages and other features of similar scale in three dimensions (3D). The chapter focuses on the use of serial sectioning methods and associated instrumentation, as this is the most widely available and accessible technique for collecting such data for the foreseeable future. Specifically, the chapter describes the serial sectioning methodology in detail, focusing in particular on automated systems that can be used for such experiments, highlights possibilities for including crystallographic and chemical data, provides a concise discussion of the post-experiment handling of the data, and identifies current shortcomings and future development needs for this field.

1 Introduction

In the previous chapter, the concept of integrated computational materials engineering (ICME) via microstructurally informed, multiscale simulations was introduced. For this type of endeavor, it is incumbent that the required microstructural information be on hand as either input or validation for these simulations to properly account for microstructural dependencies. Today, this information is most commonly found in the form of mean values for selected features, e.g., average grain size, average precipitate size or spacing, or in more advanced models, distributions of these microstructural descriptors are required.

To provide as complete and unbiased description of microstructure as possible, the field of materials characterization is gradually developing and adopting methods that provide quantitative microstructural information in three-dimensions (3D). The desire for 3D microstructural data is relatively straightforward. Primarily, it is

M.D. Uchic (✉)

Materials and Manufacturing Directorate, Air Force Research Laboratory,
Wright-Patterson Air Force Base, OH, USA

e-mail: Michael.Uchic@wpafb.af.mil

because 3D data provides access to some very important geometric and topological quantities that cannot be determined a priori by classical stereological methods that utilize only 2D images (DeHoff 1983). These quantities include assessing the true size, shape, distribution of both individual features and that of their local neighborhoods, determining the connectivity between features or networks, and counting of the number of features per unit volume (De Hoff 1983; Wolfsdorf et al. 1997).

Experimental methods that enable 3D characterization have undergone dramatic improvements in the past decade, due in large part to advances in both computing power and visualization and analysis software that have been enabling factors for both the collection and interpretation of these massive data sets. The 3D data collection process requires significantly more effort compared to conventional 2D analysis, which has spurred the development of fully automated instruments that are capable of collecting such information (Alkemper and Voorhees 2001; Spowart et al. 2003), as well as software programs that take in the raw data stack and provide as output reconstructions and analysis of the microstructural features in 3D [see for example, IMOD (Kremer et al. 1996)]. The diverse size range of microstructural features has resulted in the development of a suite of instruments to address the collection of 3D data at various size scales. This ranges from counting individual atoms in nanometer-sized needles (Miller and Forbes 2009) to interrogating features within manufactured components (MA Groeber, DM Dimiduk, MD Uchic, C Woodward 2009, unpublished research) – a difference of 7–9 orders of magnitude in scale – and cube of this value for volumetric coverage! The state-of-the-art for the field of 3D materials characterization has been the focus of recent collections of papers in a number of materials journals (Spanos 2006; Uchic 2006; Thornton and Poulsen 2008), and has also been the topic of a number of symposia at materials society meetings, for example, the 3D Materials Science symposia I to VI at the TMS national meetings.

As an aside, a similar renaissance in 3D characterization methodologies has already occurred in the biological and medical sciences, with instruments that are more suited to either sectioning soft matter, or in some cases making use of instrumentation that cannot be directly applied to opaque materials such as confocal laser microscopy. Nevertheless, the significant overlap in problems of data handling, data segmentation and feature extraction, 3D visualization, and surface meshing has accelerated the maturation of this methodology for the structural materials community.

This chapter focuses on one aspect of microstructural characterization with respect to the ICME field, which is to discuss the methodologies that can be used to quantify the 3D microstructure associated with grain ensembles or other features that are of similar scale such as second-phases, dendrites, precipitates, dispersoids, and voids. These are ubiquitous features found in most structural alloys, and these features as a whole range in size from multiple millimeters to tens-of-nanometers in scale.

There are two main experimental pathways to collect information over this size range. The first is the use of X-rays, which are nondestructive and therefore allow for time-dependent studies that examine microstructural changes due to thermal or mechanical input, i.e., 4D experiments (Juul Jensen et al. 2006). There are a number of

different techniques that can be used to provide image contrast in X-ray tomography experiments (Ice 2004). The most common method obtains information by reconstructing a suite of transmission (absorption) images taken at various projections. This technique is very sensitive to differences in atomic number and density, so that microstructural features which are quite different in these characteristics – such as porosity relative to the matrix – can be readily detected as shown in Fig. 1a. Other methods utilize diffraction contrast and either ray tracing methods (Schmidt et al. 2004; Juul Jensen et al. 2006; Ludwig et al. 2009) or other spatial localization methods (Larson et al. 2002; Ice 2006) to define features such as individual grains from grain aggregates. These diffraction-contrast methods have been greatly advanced in the past few years, and for selected techniques have been demonstrated to rapidly produce 3D characterization data of grain ensembles as shown in Fig. 1b. The primary disadvantage of these experiments is that they require the use of very high-intensity X-rays to produce data that has acceptable signal-to-noise levels, such as those produced by synchrotron sources (Ice 2004). This requirement severely restricts the general availability and applicability of these methods until there is a revolutionary change in the ability to produce high brilliance X-rays in a laboratory setting.

The other method to acquire 3D characterization data at the macro-to-microscale is through serial sectioning experiments. Serial sectioning is much more accessible experimental methodology compared to synchrotron-based tomography, but this methodology has a significant disadvantage that the sample volume is inevitably consumed during the data collection process, which precludes any re-examination or re-use of the material after analysis. In spite of this drawback, serial sectioning

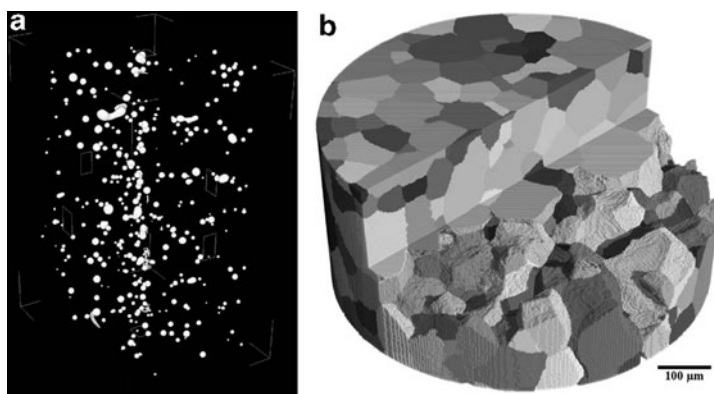


Fig. 1 Examples of microstructural data that can be obtained with synchrotron X-ray methods. (a) 3D reconstruction of the porosity in a cast single-crystal nickel base superalloy, CMSX-10, using transmission (absorption) X-ray tomography (Link et al. 2006). The dimensions of the reconstructed volume are $500 \times 500 \times 800 \mu\text{m}$. Figure is used with permission from Elsevier. (b) 3D reconstruction of the 3D grain structure of a tensile sample of β -21 titanium alloy (Ludwig et al. 2009). The reconstruction contains 1,008 grains, and was collected using X-ray differential contrast tomography. Figure is used with permission from the American Institute of Physics

experiments are becoming an increasingly common procedure to characterize microstructure in 3D, especially in the past decade with respect to the development and usage of automated instruments to perform of this task. This chapter endeavors to provide an overview of this technology, and discuss the state-of-the-art with regards to characterizing grain and precipitate scale microstructural features in structural materials.

2 Serial Sectioning

For opaque materials, serial sectioning has been the most widely used method to acquire raw 3D characterization data at the macro-to-microscale, and in fact the first application of this methodology to examine the microstructure of structural metals was published over 90 years ago ([Forsman 1918](#)). Tomographic serial sectioning experiments are conceptually simple, being composed of two steps that are iteratively repeated until completion of the experiment. The first is to prepare a nominally flat surface, which can be accomplished by a variety of methods – a noninclusive list includes cutting, polishing, ablating, etching, and sputtering – where ideally a constant depth of material removal has occurred between each section. The second step is to collect two-dimensional (2D) characterization data after each section has been prepared, although data could also be collected continually during material removal depending on the particular sectioning method that is employed. After collection of the series of 2D data files, computer software programs are used to construct a 3D array of the characterization data that can be subsequently rendered as an image or analyzed for morphological or topological parameters.

The 2D characterization data collected during a serial sectioning experiment can be comprised of number of different types and/or quantities of information. For example, in the particular case of characterizing grain microstructures, this could consist of using optical microscopy to image the structure of etched grain boundaries, as well as using an SEM to collect electron backscatter diffraction maps on key sections to characterize the average grain orientation, which was recently demonstrated by Spanos, Lewis, Rowenhorst and co-workers at the Naval Research Laboratory ([Lewis et al. 2006](#); [Spanos et al. 2008](#)), as shown in Fig. 2. From a practical perspective, the main criteria for determining whether to incorporate a particular image or data map into a serial sectioning experiment is whether the microstructural feature or features of interest can be readily classified from this information, especially via unsupervised computer segmentation processes. In the most commonly performed experiment, the characterization data consists of a single 2D image per section ([Mangan et al. 1997](#); [Kral and Spanos 1999](#); [Lund and Voorhees 2002](#); [Holzer et al. 2006](#)). Other examples include multiple images that highlight different aspects of the microstructure ([Jorgensen et al. 2009](#)), crystallographic ([Wall et al. 2001](#)) or chemical maps ([Kotula et al. 2006](#); [Schaffer et al. 2007](#)), or conceivably any other 2D spatial measurement that is of interest (such as local measurements of resistivity or elastic modulus, etc.). The process of sectioning and

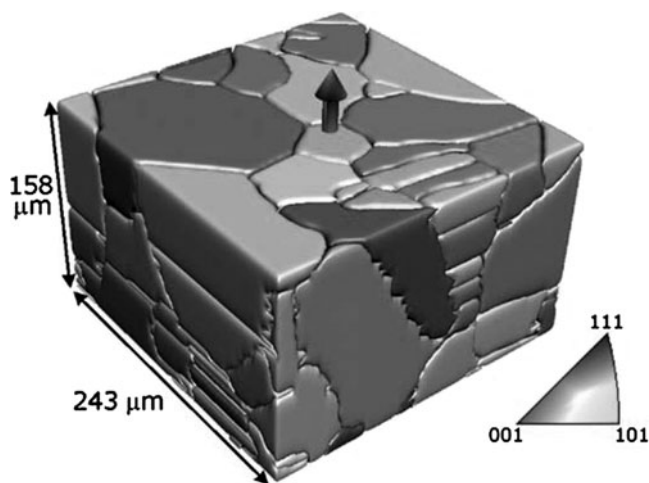


Fig. 2 3D reconstruction of the austenite phase in a commercial austenitic stainless steel alloy AL-6XN (Lewis and Geltmacher 2006). The data set was produced via manual serial sectioning that incorporated collection of both optical images and EBSD maps. The volume contains 138 grains, and the *arrow* represents the normal of the serial sectioning plane. Although not readily visible because of the gray-scale coloring of this printing, the color of each grain corresponds to the crystallographic orientation relative to the *arrow*, which was determined by EBSD. Figure is adapted with permission from Elsevier

data collection is repeated until the desired sample volume has been interrogated, or perhaps more realistically for manual implementations of this methodology, the motivation to continue collecting the data falls below a critical value.

One of the key aspects in the design of a serial sectioning experiment is to determine the minimal spatial resolution required by the subsequent microstructural analysis. For example, a serial sectioning study that will quantify aspects of feature shape such as surface area will require a much greater spatial resolution than one that is simply counting the number of features per unit volume. A rule-of-thumb is that one should strive for a minimum of ten sections per feature, although this is simply an ad hoc estimate. A better approach is to perform a critical examination of the effect that spatial resolution has on the accuracy or bias of any of the quantitative measurements-of-interest on simple test objects prior to initiating the experiment (Wojnar et al. 2004). Ideally, one would like to section at the finest possible step size and also collect high-resolution 2D data to generate the highest fidelity 3D data structures as possible. In practice, this goal is tempered by a number of factors. First, the precision of the sectioning technique should be assessed. The typical serial sectioning experiment employs a section thickness where the variability between sections is a small fraction of the total section thickness ($<10\%$), as historically most studies assume a constant section thickness and do not take this variation into account when reconstructing the data. Second, the spatial resolution of the 2D characterization technique should be considered as well.

For example, an experiment that utilizes X-ray spectroscopy via electron-beam irradiation [i.e., energy-dispersive spectroscopy (EDS) or wavelength-dispersive spectroscopy (WDS)] will have a much larger interaction volume and consequently a much poorer spatial resolution compared to an experiment that uses secondary electron imaging. Thus, the spatial resolution of each characterization technique that is employed should set a minimum bound, to prevent collecting “empty magnification” in either the 2D imaging plane or the sectioning depth. Additional feasibility issues include the proportional increase in time needed to complete a serial sectioning experiment as the spatial resolution is increased in the sectioning direction or the imaging plane, as well as the concomitant increase in computational resources for data handling and storage.

Like any experimental methodology, serial sectioning has both advantages and disadvantages. One advantage is that both sectioning equipment and 2D characterization instruments are commonly found in most materials laboratories, therefore, manual implementation of this methodology can readily be initiated, with the only significant “cost” being that of instrument and personnel time to perform this repetitious experiment. A wide variety of materials characterization methods are optimized for analysis of planar surfaces, such as light microscopy, scanning electron or ion microscopy, scanning probe microscopy or its derivatives, surface analysis techniques (EDS, XPS, Auger, SIMS, RBS, etc.), so that a wide range of materials characteristics can be obtained. The type of data that is collected during a serial sectioning experiment can have a profound impact on the ease of identifying and classifying microstructural features, and so this selection should be carefully considered in the design of the experiment. The primary disadvantage associated with this technique is the destruction of the sample, which for some applications is unacceptable. Another potential but much-less common issue is that the volume that is analyzed is always adjacent to or at the free-surface, which might affect the characterization measurement in an undesirable way.

Manual demonstrations of this experimental methodology can be found periodically throughout the 1960s to the early 2000s, and a review of these studies can be found in the papers by Kral and co-authors (Kral et al. 2000, 2004). While serial sectioning experiments can be performed in this manner, the repetitive nature of this experiment is ideally suited for automation using instruments that are designed specifically for this application. Automation clearly reduces the tedium associated with the experiment (DeHoff 1983; Kammer and Voorhees 2008), thereby providing significant gains in terms of the amount of data that can be collected. In addition, there are other potential benefits to instrument automation, such as reductions in data variability via machine inspection and metrology. For example, pattern recognition methods can be incorporated to increase the accuracy and precision of the serial section thickness (Groeber et al. 2006), or image analysis methods can be used to adjust instrument settings so that the intensity histogram or image sharpness remains unchanged throughout the experiment.

At present, there are only three devices that are capable of automatically acquiring 3D grain-level data in structural materials via serial sectioning. The next section describes these devices in some detail. Two of the devices – the Alkemper

and Voorhees micromiller and Robo-Met.3D – utilize optical microscopy as the sole characterization method. These devices have been constructed and are suitable for characterization of the microstructure of millimeter scale volumes with micron-level precision. The third device, the focused ion beam–scanning electron microscope (FIB-SEM), is not specifically designed for serial sectioning experiments, but has been adapted for this purpose through the use of machine control software scripts. This device has approximately 1–2 orders of magnitude improvement in imaging resolution as well as sectioning fidelity compared to the other serial sectioning instruments, so that micron and submicron features can be accurately characterized. Also, both crystallographic and chemical data can be collected as part of the serial sectioning experiment using commercially available detectors that can be installed on the FIB-SEM. However, this instrument cannot currently characterize larger volumes like the other two devices.

3 Automated Serial Sectioning Instrumentation

3.1 *Alkemper–Voorhees Micromiller*

This serial sectioning instrument was developed at Northwestern University by Alkemper and Voorhees (A&V) around the year 2000 ([Alkemper and Voorhees 2001](#)), to augment previous efforts by the Voorhees group ([Wolfsdorf et al. 1997](#)) to quantify materials microstructure in 3D using microtome milling, i.e., physical cutting with a rotating diamond knife. Unlike biological microtomy studies in which the thin section prepared by the cutting process is of interest, here the microtome blade is used as an end-mill to prepare an optical-quality surface in soft ductile metals and alloys that do not react adversely with the diamond blade, such as Pb, Sn, Al and Cu alloys ([Kammer and Voorhees 2008](#)). Images of this tomographic instrument are shown in Fig. 3.

At the heart of the system is a commercial microtome that is outfitted to a rotary micro-milling attachment. The microtome performs the sectioning operation by moving a sample underneath the rotating micro-milling head using a linear stage. The key improvements by A&V were to incorporate an optical microscope with a digital camera, an etching/washing/drying station, and a linear variable differential transformer (LVDT) sensor within the commercial micromiller system. The cleaning, etching, and drying station was located next to the cutting head to remove machining chips after sectioning, and also to reveal microstructural features that could be selectively attacked via chemical etching. The linear stage then translates the sample underneath the optical microscope where an image of the freshly prepared surface can be captured using a digital camera. These first two modifications eliminated the need to remove the sample from the micromiller to collect an image of the serial section surface, which resulted in significant reductions in the time needed to complete one cycle of the experiment, as well as

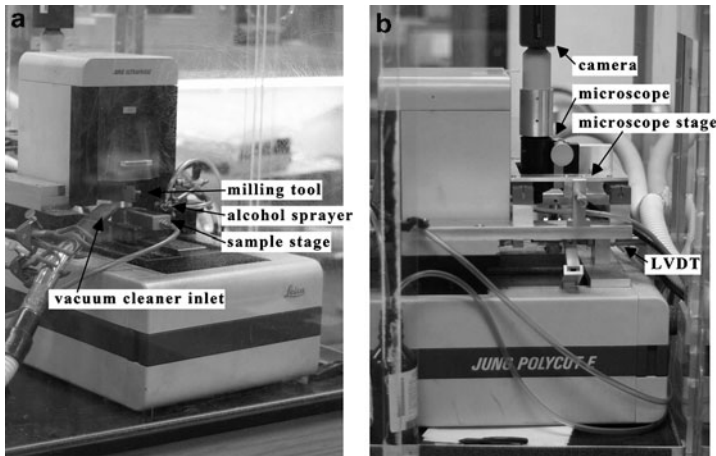


Fig. 3 The automated serial sectioning device developed by Alkemper and Voorhees (Alkemper and Voorhees 2001). (a) Image of the commercial Reichert-Jung Polycut E micromiller system, with modifications by A&V for cleaning the sample after the micromilling operation. (b) View of the microscope attachment and LVDT installed by A&V to perform automated serial sectioning. Figure is adapted from (Alkemper and Voorhees 2001) with permission from Wiley

minimizing positioning errors due to removal and subsequent re-mounting of the sample that affected the accuracy of both the cutting and imaging operations. The third modification of incorporating the LDVT allowed for an independent measurement of the spatial position of the sample when placed underneath the optical microscope. As a result, the absolute lateral position of the sample was quantitatively known for each slice, and this information was used to correct for in-plane translational errors in each of the 2D images that comprised the 3D data stack without resorting to image matching/correlation methods, which is useful in preventing alignment errors associated with using only internal features for this task (Russ 2002).

With any serial sectioning experimental methodology, one needs to quantify both the accuracy and precision of the sectioning process, as these variations lead to both systematic and random distortions in the sectioning direction of the 3D data stack. In particular, this issue is vitally important for instruments that do not monitor or measure this quantity during the experiment. The A&V micromiller utilizes a precision mechanical feed to advance the depth of the milling head over an adjustable range of 1–20 μm , but this device as constructed does not provide closed-loop control over the sectioning depth. Alkemper and Voorhees solved this problem by developing a custom calibration standard, and subsequent analysis of the 3D reconstruction of the calibration standard allowed A&V to determine that both machine errors as well as thermal expansion associated with heating of the system during operation were shown to affect the accuracy of the sectioning thickness (Alkemper and Voorhees 2001). Furthermore, they used the custom standard

to quantify the average section thickness during steady-state operation, as well as identified a minimum warm-up time for instrument operation prior to which there were significant variations in the sectioning thickness.

Examples of some of the data sets that have been collected with this device are shown in Fig. 4, which have been used to systematically quantify the dendrite coarsening process in simple binary alloy systems. The micro-milling process is fast, and optical cameras can also quickly acquire image data. As a result, this device can provide upward of 20 sections per hour, resulting in 3D data sets that are comprised of hundreds of images that are prepared in less than a day. It is clear from Fig. 4 that this device is useful for the 3D characterization of materials at the millimeter size-scale,

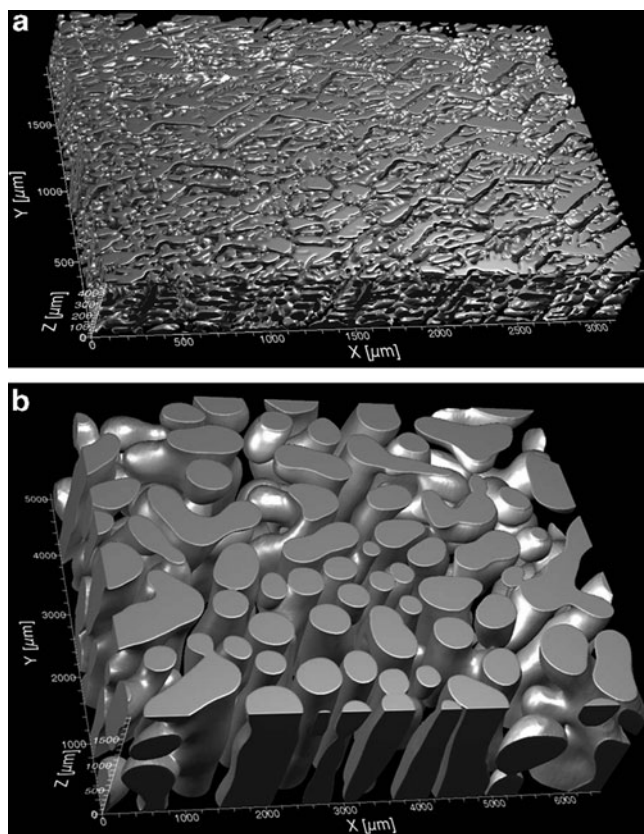


Fig. 4 Application of the A&V micromilling serial sectioning device to study dendrite coarsening processes (Kammer et al. 2006) (a) 3D reconstruction of the dendrite structure of a Pb-Sn alloy after a 3-min coarsening time. The solid corresponds to the β -Sn solid-solution dendrites, while the voids in the reconstruction correspond to the Pb-Sn eutectic phase. (b) 3D reconstruction of an Al-Cu alloy after a 3-week coarsening experiment. The solid corresponds to Al dendrites, while the voids in the reconstruction correspond to the Al-Cu eutectic phase. Note that this reconstructed volume is approximately $6 \times 5 \times 43$ mm in dimension. Figure is adapted with permission from Elsevier

as long as two conditions are met: one, the materials are compatible with diamond blade sectioning and two, the microstructural features of interest can be selectively identified from machined surfaces using only optical images and chemical etching.

3.2 *RoboMet.3D*

Another serial sectioning device, RoboMet.3D, was developed by Spowart and Mullens (Spowart et al. 2003; Spowart 2006), and an image of this system is shown in Fig. 5. This device is conceptually similar to the A&V micromiller in that there are three stations to the system – sectioning, etching/washing/drying, and optical imaging. However, the RoboMet.3D can be used to examine a much broader range of materials compared to the A&V micromiller because it uses a precision mechanical polishing system for material removal rather than micromilling. Mechanical polishing is the most commonly used method to prepare materials for metallographic analysis, and therefore the sectioning system is well suited to examining many structural materials. Each of the stations is a physically separate unit on the RoboMet.3D, and therefore a six-axis robot arm is employed to move the sample between the various stations, and also holds the sample while it is being washed, etched, and dried with forced air. Notably, the commercially available optical microscope that is used on these systems is a fully automated device in its own right, being able to perform tasks such as focusing, contrast adjustments, and the capture of large-area montages of the serial section surface without human intervention.

The sample-of-interest is mounted on a custom holder that minimizes rotational movement of the sample between polishing and imaging operations, but small lateral



Fig. 5 The automated serial sectioning device RoboMet3.D (Spowart et al. 2003; Spowart 2006). From left-to-right in the image are the precision metallographic polisher, six-axis robot, etching/washing/drying station, and a motorized inverted optical microscope. Figure is used with permission from Elsevier

translations of the sample that occur between consecutive imaging operations are not measured – these must be removed via image analysis methods as will be discussed later in this chapter. Also, RoboMet.3D does not use closed-loop control over the material removal process, but rather section-to-section consistency is maintained by keeping common variables in the polishing process fixed, such as the time of polishing, applied load, wheel speed, in addition to using fresh diamond lapping films as the polishing media. With this protocol, RoboMet.3D has been demonstrated to achieve very good control over material recession rates, with a repeatability of $\pm 0.03 \mu\text{m}$ for a section thickness of $0.8 \mu\text{m}$ (Spowart 2006).

The device can prepare sections ranging from ~ 0.1 to $10 \mu\text{m}$ in thickness and complete the sectioning cycle up to 20 times per hour (Spowart 2006), where the cycle time is mostly dependent on the sectioning depth, the etching time needed to resolve the feature-of-interest, and the on the quantity, resolution, and number of images that are acquired per section. Figure 6 shows representative data from the RoboMet.3D that highlights the good volumetric coverage that can be obtained with this device, as well as the diversity of materials that can be examined with this instrument. Like the A&V micromiller, this device can be successfully employed if two conditions are met: one, that a single polishing step provides both adequate material removal rates and sufficient metallographic surface quality and two, the microstructural features of interest can be identified using optical imaging methods.

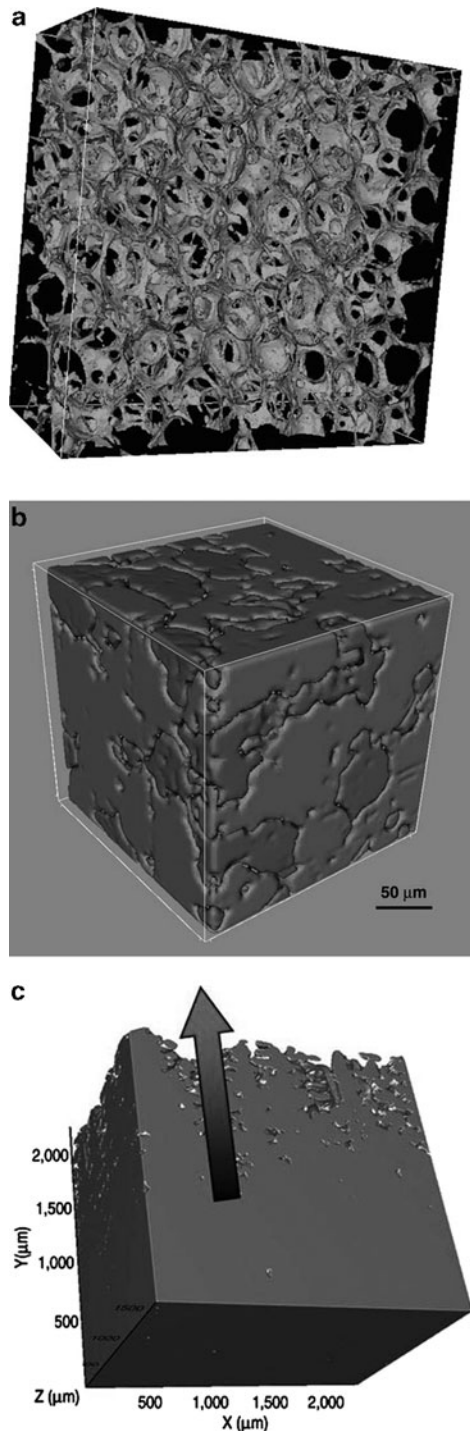
3.3 *Focused Ion Beam–Scanning Electron Microscopes*

For smaller-scale grain and precipitate structures – those that are approximately $10 \mu\text{m}$ in scale or smaller – FIB-SEM are well suited to characterize these features in 3D via serial sectioning (Dunn and Hull 1999; Inkson et al. 2001; Uchic et al. 2006, 2007). FIB columns are able to focus highly energetic ions (typically Ga^+) to small spot sizes that are on the order of $5\text{--}20 \text{ nm}$. The interaction of these energetic ions with a target results in localized material removed via ion sputtering interactions (Orloff et al. 2003). FIB microscopes are well suited to perform serial sectioning via cross-section milling with extremely fine resolution, and at the extreme can provide average serial section thickness of approximately $10\text{--}15 \text{ nm}$ using closed-loop control measures (Bansal et al. 2006; Holzer et al. 2006). This value is at least one order of magnitude finer than the section thickness that can be nominally achieved with traditional mechanical removal methods such as metallographic polishing. Using the appropriate software control scripts, a typical serial sectioning experiment will usually encompass material volumes that are larger than $1,000 \mu\text{m}^3$ with voxel dimensions approaching tens-of-nanometers. This combination of spatial coverage and resolution cannot be achieved with any other tomographic instrument.

FIB-SEM microscopes have other advantages relative to the task of serial sectioning. Cross-section ion milling is an almost universally applicable method for

Fig. 6 Examples of 3D data sets that have been produced using RoboMet3.D.

(a) Iso-surface rendering of a structural carbon foam (Maruyama et al. 2006). Dimensions of the 3D reconstruction are $1,526 \times 1,526 \times 776 \mu\text{m}$, and the average serial section thickness is $3.5 \mu\text{m}$. Figure is used with permission from Elsevier. (b) 3D reconstruction of a powder-compacted Fe-Cu alloy, which utilized an average serial section thickness of $1.2 \mu\text{m}$ (Spowart 2006). Figure is used with permission from Elsevier. (c) 3D reconstruction of the mushy zone during directional solidification of a commercial cast single crystal Ni-base superalloy René N4 (Madison et al. 2008), which utilized an average serial section thickness of $2.2 \mu\text{m}$. Figure is used with permission from Springer



preparing planar surfaces, and has been successfully applied to metallic alloys, ceramics, polymers, electronic materials and biological materials, although for some systems both low beam currents and sample cooling are required to prevent alteration of the starting microstructure. In comparison with most polishing or cutting methods, ion sputtering is a relatively low damage process that not only preserves the details of hard-to-prepare microstructures like those composed of both soft and hard phases, or brittle materials that contain significant porosity, but the depth of the damage layer is small enough to permit the usage of surface-damage sensitive techniques like electron backscattered diffraction (EBSD) for selected metallic alloys (Groeber et al. 2006; Konrad et al. 2006; Zaefferer et al. 2008).

One other significant advantage of FIB-SEM microscopes is ability to incorporate imaging and surface analysis methodologies that can greatly mitigate the difficulty in classifying various microstructural features like grains and precipitates. These characterization methods include high-resolution backscattered electron (BSE) images that exhibit atomic-number contrast to differentiate between multiple phases, ion-induced secondary electron (ISE) images that often exhibit channeling contrast which can differentiate individual grains in polycrystalline materials (Orloff et al. 2003), EBSD mapping for local crystallographic orientation measurements, and EDS (Kotula et al. 2006), WDS, or secondary ion mass spectroscopy (SIMS) (Dunn and Hull 1999) for local chemical spectra mapping. The information limits for these methods are often of the same order of magnitude as the FIB sectioning capabilities, thus a properly outfitted microscope can provide the user tremendous flexibility in selecting which types of structural, chemical, or crystallographic information are important for their particular characterization study. For example, if only structural information is required, then image data may suffice. Chemical or crystallographic analysis can be included to help with the identification of particular phases and grain orientations, respectively.

The procedure for performing an automated FIB-SEM serial sectioning experiment is roughly similar to the methods that use bulk sectioning processes. First the sample volume-of-interest is initially prepared, as FIB serial sectioning experiments have some specific sample geometries that can improve the quality of data that is collected (Uchic et al. 2006, 2007). Next, software control scripts are used to move the sample between sectioning and characterization steps. In their most basic form, these scripts perform the primary functions of cross-section ion milling of the sample and collection of electron images, as shown in Fig. 7. For these experiments, the sample does not need to move if it is placed at a position where both electron and ion columns can simultaneously image the same region of the sample, which greatly simplifies both the experimental setup and the complexity of the control scripts required to automate the experiment. Like the other serial sectioning instruments discussed previously, the use of machine control scripts allows for a more consistent serial slice thickness, reduces the time needed per acquisition cycle, and enables the microscopes to run unattended for periods of about 1–2 days. More advanced control scripts incorporate image recognition procedures to minimize the effects of electrical, thermal, or mechanical drift, as well as to incorporate a wider range of data signals like ISE imaging or EBSD mapping, which requires accurate sample

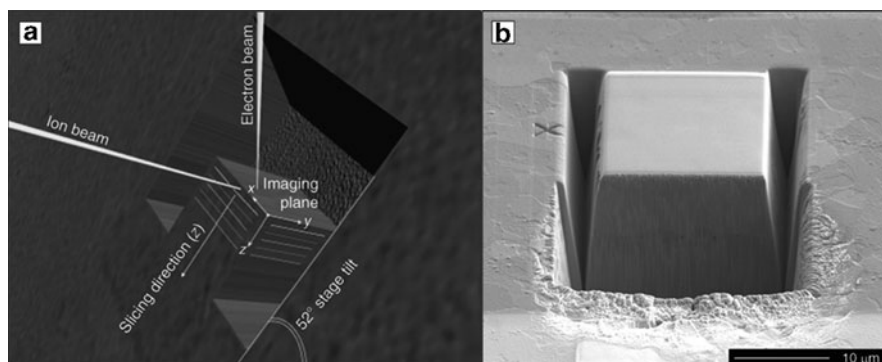


Fig. 7 The standard sample geometry and its orientation within a FIB-SEM microscope for a typical serial sectioning experiment (Holzer et al. 2006; Uchic et al. 2007). (a) Schematic of the experimental set-up for an FIB-SEM serial sectioning experiment where cross-section ion milling is used to controllably remove material at the micro- to nanoscale, and electron imaging is used to characterize the freshly prepared surface. If only electron imaging or EDS is used to characterize the sample surface, then the sample does not need to be moved during the tomographic experiment. (b) SEM image of a sample volume prior to sectioning. The trenches that surround the sample volume allow the electron beam to image the serial-sectioned surface, and also help prevent sputtered and re-deposited material from obscuring the surface-of-interest. Figure is used with permission from the Materials Research Society

repositioning after complex five-axis stage movements (Groeber et al. 2006). Note that for the experiments that use image recognition methods, these microscopes provide closed-loop control over sectioning thickness (unlike the two previously described serial sectioning instruments), thus enabling the user to simply select the serial sectioning depth and eliminating the need for calibration runs.

Commercial FIB-SEM instrumentation is installed in many laboratories worldwide, and therefore this system is the most widely used of the three automated serial sectioning systems discussed in this chapter. Figure 8 shows representative examples of 3D data that have been collected with these instruments, which highlights the diversity of size scales that can be examined (Fig. 8a), the ability to characterize precipitate- and multiple-phase microstructures at the microscale (Figs. 8b, c), and the ability to examine grain-level microstructures that includes the automated collection of orientation information (Fig. 8d). This figure demonstrates that FIB-SEM microscopes epitomize a new breed of multimodal serial sectioning instruments, as they are currently capable of high-fidelity characterization of the morphology, crystallography, and chemistry of micron and submicron size features in 3D. One final note is that these experiments can require significant instrument time to complete an experiment depending on the size of the volume that is examined and the type of data that is collected. Although some experiments require only a few hours – like those where the milling step takes a couple of minutes to execute, and a single electron image is collected for each section – others that include chemical or crystallographic maps, or those that attempt to interrogate volumes that have submillimeter dimensions may require multiple days.

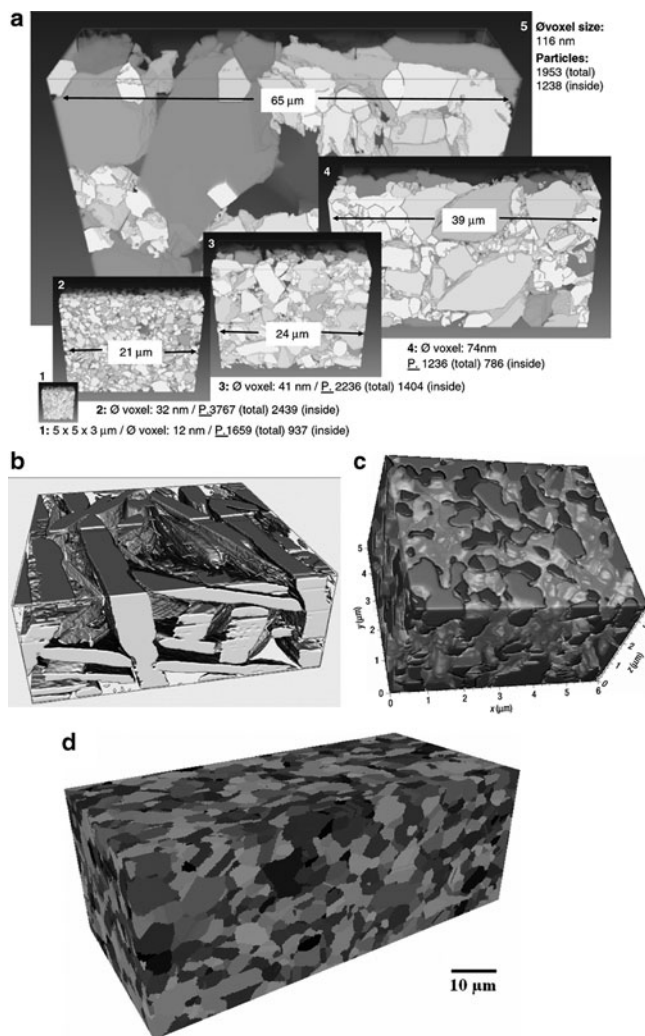


Fig. 8 Representative examples of 3D reconstructions that have been collected using a dual beam FIB-SEM. **(a)** Five reconstructions of portland cement agglomerants where the average particle size is different in each reconstruction, ranging from 0.68 to 14.2 µm (Holzer et al. 2006). The voxel edge length as well as the number of particles identified in each volume is listed next to each reconstruction. Figure is used with permission from Wiley. **(b)** Reconstruction of α -laths from a Ti-6242 colony (Simmons et al. 2009). Figure is used with permission from the IOP. **(c)** Anode of a solid-oxide fuel cell, which is composed of three phases: Ni (light gray), pores (dark gray), and yttria-stabilized zirconia (translucent phase) (Wilson et al. 2006). Figure is used with permission from the Nature Publishing Group. **(d)** A 3D reconstruction of the grain structure from a powder-metallurgy Ni-based superalloy, IN100. The volume shown has dimension of $96 \times 36 \times 46$ µm with a voxel edge length of 250 nm, and EBSD data was used to form this reconstruction, which provided information on both the morphology and crystallography of the grain structure (Groeber et al. 2008). Figure is used with permission from Elsevier

4 Data Processing and Segmentation

After completion of the serial sectioning experiment using either manual or automated methods, the stack of 2D data files need to be combined and processed in such a way so that the microstructural features that are within the 3D data stack can be classified. Said differently, for each object of interest in the data, i.e., every grain, precipitate, dendrite, void, and so on, one has to identify all of the voxels that are associated with that object. This procedure is referred to as data segmentation. Once all of the objects and their voxels are identified and classified, the process of quantifying microstructural characteristics using computational methods can be readily performed; this topic is the subject of other chapters in this book, and therefore will not be covered here.

While the concepts of segmentation and classification is straightforward – as humans we perform this task during every waking moment – in practice this can be the toughest and often rate-limiting step to transforming the serial sectioning data into a useful form. The difficulty with data segmentation is utterly dependent on the type, quantity, and quality of data from the serial sectioning experiment, as well as the complexity of the microstructure of the material being examined. This is especially true for serial sectioning experiments that only collect image data, because of the general difficulty in using semi- or fully automated computer segmentation algorithms to defining objects from visually complex images. Note that unsupervised computerized segmentation processes are a necessary component of tomographic experiments because of the sheer volume of information that is contained within the data sets, thus eliminating the possibility of human-assisted segmentation except when only a handful of features require classification.

A necessary step (typically performed before image segmentation) is to ensure that the spatial registry of each 2D data file that collectively comprises the 3D data stack is accurate. Each data file may have to be translated, stretched, rotated, or possibly all three in combination to account for the fact that the sample may have been in different physical locations when the 2D characterization data was collected, to correct for systematic or random distortions that may have also occurred during data collection (for example, image foreshortening), or to overlay data that may have been acquired at different spatial resolutions. The need for data alignment and registration is extremely common for most tomographic experiments, although manually performed experiments generally have more section-to-section variability unless specific measures such as dedicated sample fixtures are employed. One solution is to have an independent record of the spatial position of the sample relative to the 2D characterization device during data collection, like the LVDT data used in the A&V micromilling device. However, most tomographic instruments do not have the capability to provide this information at the present time.

Another method to perform data alignment is through the use of fiducial markers that are within or on the outside of the sample volume. A commonly used method is the use of multiple hardness indentations ([Kral and Spanos 1999](#)). As long as the indentations are relatively large so that their shape is not grossly changed between consecutive sections, these markers not only provide an independent reference to adjust for any in-plane affine transformation of the data, but also the relative change

of the diameter of the indent from section-to-section provides a local gage of the sectioning depth that can be used to correct for the position of the data along the sectioning direction within the 3D stack. Other fiducial marker strategies have also been proposed, involving machining patterns directly onto the side of the sample (Spanos et al. 2008) or onto a chip that is glued to the sample (Wall et al. 2001) that also provide both in-plane and depth removal information.

A third option is to simply use the internal features that are present in the data for registration, but this method can introduce systematic errors unless the microstructure is relatively isotropic (Russ 2002). There are a number of signal processing algorithms that can be used for spatial alignment. Cross-correlation or other convolution methods are very commonly used if the data that is being registered is very similar from slice to slice, for example, image data that has approximately the same intensity and brightness variations throughout the data stack (Gulsoy et al. 2008). There are newer techniques such as mutual information (Pluim et al. 2003) that can also be used for this purpose, which is especially helpful in registering different forms of data, such as combining images with chemical or crystallographic maps (Gulsoy et al. 2008).

After correcting for spatial registry, another common operation is to use interpolation methods to adjust the x-y resolution of the 2D data files to match the average sectioning depth, to produce cubic voxels for the 3D array. Finally, one usually selects a subregion from the 3D array, to define a volume that eliminate areas that have poor data quality or other artifacts, and if needed, to minimize the size of the data volume to prevent problems with computer memory allocation.

The next step after data alignment is data segmentation, which Gonzales and Woods define for an image as “subdividing an image into its constituent regions or objects” (Gonzales and Woods 2002). For example, let us consider a two-phase microstructure that consists of a matrix with precipitates, as shown in Fig. 9. If one can obtain images of this structure that display a large contrast difference between

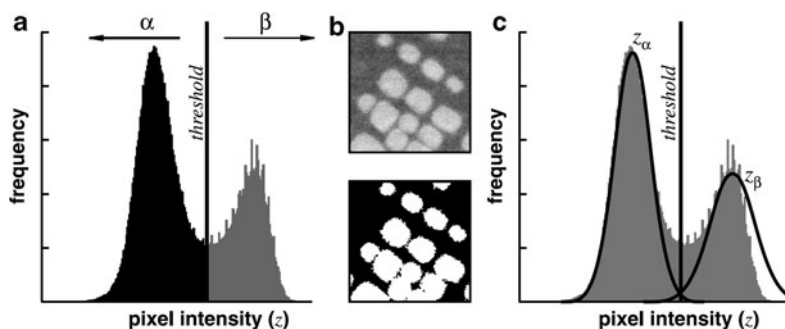


Fig. 9 (a) Intensity histogram for the ISE image shown in the upper frame of (b), which is of γ' precipitates from a Ni-based superalloy. For this histogram, the threshold value that correctly separates the pixels associated with γ' from the matrix can be readily drawn by eye, or determined analytically by fitting the intensity histogram to two Gaussian peaks (c). The application of this threshold can be seen in the lower frame of (b). Figure is used with permission from the IOP (Simmons et al. 2009)

the two phases and the contrast/brightness levels are maintained throughout the experiment, data segmentation might consist only of a single threshold operation for the entire 3D stack. Unfortunately, the complexity found in most microstructures and/or limitations of the experimental data often makes life much more difficult! The combined subject of signal processing of images and its relationship to image segmentation is far too complex to cover even in brief detail in this chapter, as there are textbooks written to examine this subject (Gonzales and Woods 2002; Russ 2002). Rather, the reader is encouraged to review these resources, and this discussion will restrict its comments to the following two recommendations to help ameliorate this process.

The first recommendation is in spite of the fact that the algorithms for performing image segmentation are becoming ever more sophisticated, especially for problems encountered in materials characterization [see for example (Jorgensen et al. 2009; Simmons et al. 2009)], there is no substitution for optimizing the “quality” of image data (Russ 2002). In particular, the experimentalist should strive to find an imaging condition or perhaps multiple imaging conditions that enable simple signal processing operations to readily threshold the features-of-interest. A recent example of this strategy is highlighted in the paper by Wilson et al. (2009), who utilized energy-biased low-kV backscattered images to readily define the various phases observed in solid-oxide fuel cell cathodes.

The second recommendation is to consider incorporating crystallographic or chemical maps rather than only image data, even though the amount of time needed to complete the experiment is usually significantly greater when these techniques are included. For the particular problem of characterizing grain structures, one method that is very attractive is to collect orientation information during the tomographic experiment, such as EBSD maps. The commercial manufacturers that supply such instrumentation have already developed a segmentation and analysis methodology to convert the Kikuchi band pattern generated by the interaction of the electron beam with the sample into a crystallographic orientation. Thus, the “difficult” part of image segmentation has already been solved, and more importantly, the singular characteristic that defines a grain – common crystallographic orientation – is an inherent part of the data collected during the experiment. The studies of Groeber (Groeber et al. 2006, 2008) and Zaefferer (Konrad et al. 2006; Zaefferer et al. 2008) have demonstrated that grain structures can be readily defined using this methodology. Similar comments hold as well for chemical spectra image data, especially when used in conjunction with automated phase analysis software, such as that developed by Kotula et al. (2003).

5 Summary Comments: Future Developments and Needs

The serial sectioning methodologies and new experimental instrumentation shown in this chapter demonstrate a direct pathway to collecting and providing 3D data for both grain and precipitate structures. However, these achievements have only

partially completed the anticipated ICME need for fully autonomous systems that can provide a complete description of microstructural distributions from the micro-to-macro scale. The necessity for autonomous systems is driven by both the inherent statistical nature of microstructural arrangements and the accelerated pace of twenty-first century research programs.

For serial sectioning devices that operate at the millimeter scale, current automated instrumentation allows one to readily acquire structural information of grain-level microstructures via optical imaging techniques and simple mechanical removal methods, but collection of other basic information such as crystallographic or chemical information requires manual intervention. At the microscale, there is a greater quantity of spectral information that can be currently integrated into automated FIB-SEM data collection processes, via either electron or ion imaging and their derivatives, or chemical or crystallographic mapping.

This chapter concludes with a list of future instrumentation and other advancements from the author's perspective that should make for significant improvements in performing robust serial sectioning experiments, and ultimately make a positive impact in the field of ICME:

- Automated serial sectioning instrumentation that provides both high-spatial resolution (nanometer-to-submicrometer voxels) and multimodal data collection that is also capable of interrogating millimeter scale and larger volumes. One example of such instrumentation would be to integrate fine-scale macroscale sectioning methods with an SEM outfitted with the current state-of-the-art EBSD and silicon-drift-detector EDS systems.
- Extending mechanical or other macroscale sectioning methods like ultrafast laser-ablation (Echlin and Pollock 2008) to enable automated characterization of coarse microstructural features within full-scale engineering components.
- Further incorporation of machine inspection and metrology tools to improve both the repeatability and accuracy of the sectioning process and the task of image stack registration.
- Improved multimodal data collection. For example, the ability to simultaneously collect both chemical and crystallographic data for automated phase analysis has already been commercialized for 2D data collection using electron microscopes (e.g., the Pegasus and Trident systems by EDAX, Inc, or the INCASynergy system by Oxford Instruments). However, the capability to perform similar data acquisition outside a high-vacuum environment remains to be demonstrated.
- Continued improvement in data segmentation algorithms.
- Real-time analysis and feedback to the characterization subsystems with respect to feature segmentation and classification during data acquisition. To the author's knowledge, almost every tomographic experiment is performed asynchronously, that is, the data collection process is performed independently of data segmentation and classification. However, real-time interaction between the analysis software and characterization instruments would be especially useful for destructive techniques such as serial sectioning. One can envision that this capability would help ensure that all features within the analysis area would be positively

identified before proceeding to the next section. Also, experimental acquisition times should be significantly reduced if the tomographic instrument collected information only at the location and frequency with which it is needed.

References

- Alkemper J, Voorhees PW (2001) Quantitative serial sectioning analysis. *J Microsc* 201:388–394
- Bansal RK, Kubis A, Hull R, Fitz-Gerald JM (2006) High-resolution three-dimensional reconstruction: a combined scanning electron microscope and focused ion-beam approach. *J Vac Sci Technol B* 24(2):554–561
- DeHoff RT (1983) Quantitative serial sectioning analysis: preview. *J Microsc* 131:259–263
- Dunn DN, Hull R (1999) Reconstruction of three-dimensional chemistry and geometry using focused ion beam microscopy. *Appl Phys Lett* 75:3414–3416
- Echlin M, Pollock T (2008) Femtosecond Laser Serial Sectioning: A New Tomographic Technique. WCCM8/ECCOMAS
- Forsman O (1918) Undersökning av rymdstrukturen hos ett kolstä av hypereutektoid sammansättning. *Jernkontorets Ann* 102:1–30
- Gonzales RC, Woods RE (2002) *Digital Image Processing*, 2nd edn. Prentice Hall, Upper Saddle River, NJ
- Groeber MA, Haley BK, Uchic MD, Dimiduk DM, Ghosh S (2006) 3D reconstruction and characterization of polycrystalline microstructures using a FIB-SEM system. *Mater Char* 57:259–273
- Groeber MA, Ghosh S, Uchic MD, Dimiduk DM (2008) A framework for automated analysis and simulation of 3D polycrystalline microstructures. Part I: statistical characterization. *Acta Mater* 56:1257–1273
- Gulsoy EB, Simmons JP, De Graef M (2008) Application of joint histogram and mutual information to registration and data fusion problems in serial sectioning microstructure studies. *Scripta Mater* 60:381–384
- Holzer L, Muench B, Wegmann M, Gasser P, Flatt R (2006) FIB-nanotomography of particulate systems—Part I: particle shape and topology of interfaces. *J Am Ceram Soc* 89:2577–2585
- Ice GE (2004) X-ray microtomography. In: Vander Voort GF (ed) *ASM Handbook*, Vol. 9, Metallography and Microstructure, pp. 461–464. ASM International, Materials Park, OH
- Ice GE, Pang JW, Barabash RI, Puzrev Y (2006) Characterization of three-dimensional crystallographic distributions using polychromatic X-ray microdiffraction. *Scripta Mater* 55:57–62
- Inkson BJ, Mulvihill M, Möbus G (2001) 3D determination of grain shape in a FeAl-based nanocomposite by 3D FIB tomography. *Scripta Mater* 45:753–758
- Jorgensen PS, Hansen KV, Larsen R, Bowen JR (2009) A framework for automated segmentation in three dimensions of microstructural tomography data. *Ultramicroscopy*. doi: 10.1016/j.ultramicro.2009.11.013
- Juul Jensen D, Lauridsen EM, Margulies L, Poulsen HF, Schmidt S, Sorensen HO, Vaughan GBM (2006) X-ray microscopy in four dimensions. *Mater Tod* 9:18–25
- Kammer D, Mendoza R, Voorhees PW (2006) Cylindrical domain formation in topologically complex structures. *Scripta Mater* 55:17–22
- Kammer D, Voorhees PW (2008) Serial sectioning and phase-field simulations. *MRS Bull* 33:603–610
- Kotula PG, Keenan MR, Michael JR (2003) Automated analysis of SEM X-ray spectral images: a powerful new microanalysis tool. *Microsc Microanal* 9:1–17
- Kotula PG, Keenan MR, Michael JR (2006) Tomographic spectral imaging with multivariate statistical analysis: comprehensive 3D microanalysis. *Microsc Microanal* 12(1):36–48
- Konrad J, Zaefferer S, Raabe D (2006) Investigation of orientation gradients around a hard Laves particle in a warm-rolled Fe₃Al-based alloy using a 3D EBSD-FIB technique. *Acta Mater* 54:1369–1380

- Kral M, Spanos G (1999) Three-dimensional analysis of proeutectoid cementite precipitates. *Acta Mater* 47:711–724
- Kral MV, Mangan MA, Rosenberg RO, Spanos G (2000) Three-dimensional analysis of microstructures. *Mater Charact* 45:17–23
- Kral MV, Ice GE, Miller MK, Uchic MD, Rosenberg RO (2004) Three dimensional microscopy. In: Vander Voort GF (ed) *ASM Handbook, Vol. 9, Metallography and Microstructure*. ASM International, Materials Park, OH
- Kremer JR, Mastronarde DN, McIntosh JR (1996) Computer visualization of three-dimensional image data using IMOD. *J Struct Biol* 116:71–76
- Larson BC, Yang W, Ice GE, Budai JD, Tischler JZ (2002) Three-dimensional X-ray structural microscopy with submicrometre resolution. *Nature* 415:887–890
- Lewis AC, Bingert JF, Rowenhorst DJ, Gupta A, Geltmacher AB, Spanos G (2006) Two- and three-dimensional microstructural characterization of a super-austenitic stainless steel. *Mater Sci Eng A* 418:11–18
- Lewis AC, Geltmacher AB (2006) Image-based modeling of the response of experimental 3D microstructures to mechanical loading. *Scripta Mater* 55:81–85
- Link T, Zabler S, Epishin A, Haibel A, Bansal M, Thibault X (2006) Synchrotron tomography of porosity in single-crystal nickel base superalloys. *Mat Sci Eng A* 425:47–54
- Ludwig W, Reischig P, King A, Herbig M, Lauridsen EM, Johnson G, Marrow TJ, Buffiere JY (2009) Three-dimensional grain mapping by x-ray diffraction contrast tomography and the use of Friedel pairs in diffraction data analysis. *Rev Sci Instrum* 80:033905
- Lund AC, Voorhees PW (2002) The effect of elastic stress on microstructural development: the three-dimensional microstructure of a γ - γ' alloy. *Acta Mater* 50:2585–2598
- Madison J, Spowart JE, Rowenhorst DJ, Pollock TM (2008) The three-dimensional reconstruction of the dendrite structure at the solid-liquid interface of a Ni-based single crystal. *JOM* 60(7): 26–30
- Mangan MA, Lauren PD, Shiflet GJ (1997) Three-dimensional reconstruction of Widmanstätten plates in Fe-123Mn-08C. *J Microsc* 188:36–41
- Maruyama B, Spowart JE, Hooper DJ, Mullins HM, Druma AM, Druma C, Alam MK (2006) A new technique for obtaining three-dimensional structures in pitch-based carbon foams. *Scripta Mater* 54:1709–1713
- Miller MK, Forbes RG (2009) Atom probe tomography. *Mater Charact* 60:461–469
- Orloff J, Utlaut M, Swanson L (2003) *High Resolution Focused Ion Beams: FIB and Its Applications*. Kluwer Academic/Plenum, New York
- Pluim JPW, Maintz JBA, Viergever MA (2003) Mutual information based registration of medical images: a survey. *IEEE Trans Med Imaging* 22:986–1004
- Russ JC (2002) *The Image Processing Handbook*, 4th edn. CRC Press, Boca Raton, FL
- Schaffer M, Wagner J, Schaffer B, Schmied M, Mulders H (2007) Automated three-dimensional X-ray analysis using a dual-beam FIB. *Ultramicroscopy* 107:587–597
- Schmidt S, Nielsen SF, Gundlach C, Margulies L, Huang X, Juul Jensen D (2004) Watching the growth of bulk grains during recrystallization of deformed metals. *Science* 305:229–232
- Simmons JP, Chuang P, Comer M, Spowart JE, Uchic MD, De Graef M (2009) Application and further development of advanced image processing algorithms for automated analysis of serial section image data. *Mod Sim Mater Sci Eng* 17:025002–0250024
- Spanos G (2006) Foreword: scripta materialia viewpoint set on 3D characterization and analysis of materials. *Scripta Mater* 55:3
- Spanos G, Rowenhorst DJ, Lewis AC, Geltmacher AB (2008) Combining serial sectioning, EBSD analysis, and image-based finite element modeling. *MRS Bull* 33:597–602
- Spowart JE (2006) Automated serial sectioning for 3-D analysis of microstructures. *Scripta Mater* 55:5–10
- Spowart JE, Mullens HM, Puchala BT (2003) Collecting and analyzing microstructures in three dimensions: a fully automated approach. *JOM* 55:35–37
- Thornton K, Poulsen HF (2008) Three-dimensional materials science: an intersection of three-dimensional reconstructions and simulations. *MRS Bull* 33:587–595

- Uchic MD (2006) 3D microstructural characterization: methods, analysis, and applications. *JOM* 58:24
- Uchic MD, Groeber MA, Dimiduk DM, Simmons JP (2006) 3D microstructural characterization of nickel superalloys via serial-sectioning using a dual beam FIB-SEM. *Scripta Mater* 55:23–28
- Uchic MD, Holzer L, Inkson BJ, Principe EL, Munroe P (2007) Three-dimensional microstructural characterization using focused ion beam tomography. *MRS Bull* 32:408–416
- Wall MA, Schwartz AJ, Nguyen L (2001) A high-resolution serial sectioning specimen preparation technique for application to electron backscatter diffraction. *Ultramicroscopy* 88:73–83
- Wilson JR, Kobsiriphat W, Mendoza R, Chen HY, Hiller JM, Miller DJ, Thornton K, Voorhees PW, Adler SB, Barnett SA (2006) Three-dimensional reconstruction of a solid-oxide fuel-cell anode. *Nat Mater* 5:541–544
- Wilson JR, Duong AT, Gameiro M, Chen HY, Thornton K, Mumm DR, Barnett SA (2009) Quantitative three-dimensional microstructure of a solid oxide fuel cell cathode. *Electrochem Commun* 11:1052–1056
- Wojnar L, Kurzydowski JK, Szala J (2004) Quantitative image analysis. In: Vander Voort GF (ed) *ASM Handbook*, Vol. 9, Metallography and Microstructure. ASM International, Materials Park, OH
- Wolfsdorf TL, Bender WH, Voorhees PW (1997) The morphology of high volume fraction solid-liquid mixtures: an application of microstructural tomography. *Acta Mater* 45:2279–2295
- Zaefferer S, Wright SI, Raabe D (2008) Three-dimensional orientation microscopy in a focused ion beam-scanning electron microscope: a new dimension of microstructural characterization. *Metall Mater Trans A* 39A:374–389

Computational Methods for Microstructure-Property
Relationships

Ghosh, S.; Dimiduk, D. (Eds.)

2011, XVII, 658 p., Hardcover

ISBN: 978-1-4419-0642-7